

Metallomics

Accepted Manuscript



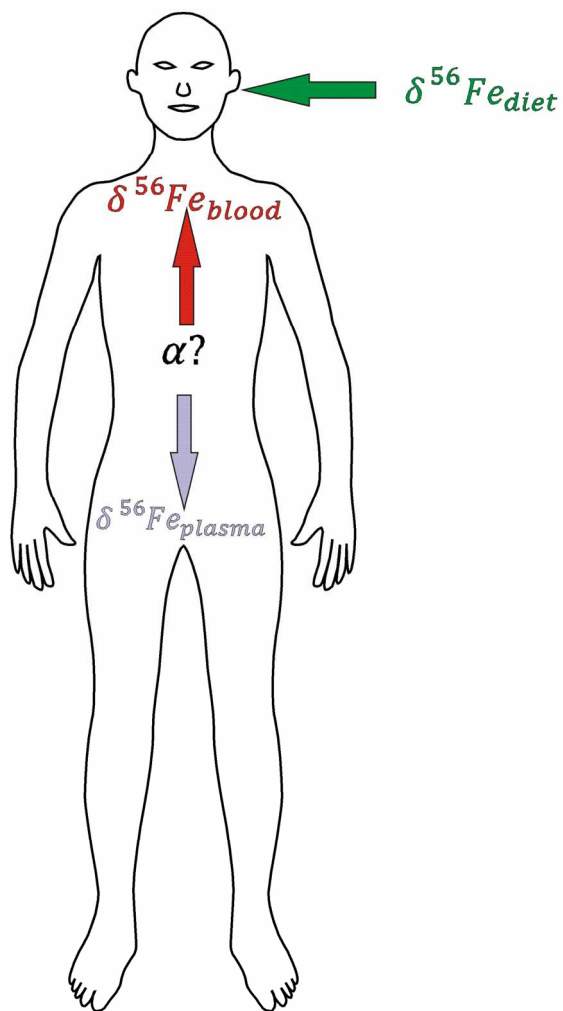
This is an *Accepted Manuscript*, which has been through the Royal Society of Chemistry peer review process and has been accepted for publication.

Accepted Manuscripts are published online shortly after acceptance, before technical editing, formatting and proof reading. Using this free service, authors can make their results available to the community, in citable form, before we publish the edited article. We will replace this *Accepted Manuscript* with the edited and formatted *Advance Article* as soon as it is available.

You can find more information about *Accepted Manuscripts* in the [Information for Authors](#).

Please note that technical editing may introduce minor changes to the text and/or graphics, which may alter content. The journal's standard [Terms & Conditions](#) and the [Ethical guidelines](#) still apply. In no event shall the Royal Society of Chemistry be held responsible for any errors or omissions in this *Accepted Manuscript* or any consequences arising from the use of any information it contains.

$$\delta^{56}\text{Fe} = \frac{(^{56}\text{Fe}/^{54}\text{Fe})_{\text{sample}}}{(^{56}\text{Fe}/^{54}\text{Fe})_{\text{standard}}} - 1$$



Iron stable isotopes can be measured precisely with multicollector ICP-MS. These stable isotope ratios change during iron uptake and metabolism due to isotope effects associating the chemical reactions of iron processing in the body. Here we explore whether the ratios fractionate between human blood and human blood plasma.

95x188mm (300 x 300 DPI)

Cite this: DOI: 10.1039/c0xx00000x

www.rsc.org/xxxxxx

Full Paper

An iron stable isotope comparison between human erythrocytes and plasma

Friedhelm von Blanckenburg ^{a,b}, Marcus Oelze ^{a,b}, Dietmar G. Schmid ^c, Kirsten van Zuilen ^{a,d}, Hans-Peter Gschwind ^c, Alan J. Slade ^e, Sylvie Stitah ^f, Daniel Kaufmann, ^g and Piet Swart ^c

Received (in XXX, XXX) Xth XXXXXXXXXX 20XX, Accepted Xth XXXXXXXXXX 20XX

DOI: 10.1039/b000000x

We present precise iron stable isotope ratios measured by multicollector-ICP mass spectrometry (MC-ICP-MS) of human red blood cells (erythrocytes) and blood plasma from 12 healthy male adults taken during a clinical study. The accurate determination of stable isotope ratios in plasma first required substantial method development work, as minor iron amounts in plasma had to be separated from a large organic matrix prior to mass-spectrometric analysis to avoid spectroscopic interferences and shifts in the mass spectrometer's mass-bias. The $^{56}\text{Fe}/^{54}\text{Fe}$ ratio in erythrocytes, expressed as permil difference to the "IRMM-014" iron reference standard ($\delta^{56/54}\text{Fe}$) ranges from -3.1‰ to -2.2‰; a range typical for male Caucasian adults. The individual subject erythrocytes' iron isotope composition can be regarded as uniform over the 21 days investigated, as variations (± 0.059 to $\pm 0.15\text{‰}$) are mostly within analytical precision of reference materials. In plasma, $\delta^{56/54}\text{Fe}$ values measured in two different laboratories range from -3.0‰ to -2.0‰, and are on average 0.24‰ higher than those in erythrocytes. However, this difference is barely resolvable within one standard deviation of the differences (0.22‰). Taking into account possible contamination due to hemolysis (iron concentrations are only 0.4 to 2 ppm in plasma compared to approx. 480 ppm in erythrocytes), we model the pure plasma $\delta^{56/54}\text{Fe}$ to be on average 0.4‰ higher than that in erythrocytes. Hence, the plasma iron isotope signature lies between that of the liver and that of erythrocytes. This difference can be explained by redox processes involved during cycling of iron between transferrin and ferritin.

Introduction

The stable isotopes of iron bear potential to serve as biomarkers for metabolic processes in humans¹. The introduction of multicollector inductively-coupled-mass spectrometers (MC-ICP-MS) about 15 years ago (see² for a review) has enabled disclosing this potentially rich reservoir of information on nutrient uptake paths, processes, and efficiencies³. Concerning the stable isotopes of iron, it is now well-established that the human blood and muscle tissue enriches the stable isotope of ^{54}Fe by one to two permil [‰] over ^{56}Fe when compared to the human diet^{1, 3-4}. However, the light iron isotopes are distributed unevenly: blood was found to contain the lightest composition, whereas the liver was less enriched in ^{54}Fe ¹. This picture was confirmed by a pig model study⁵ and by observations in mice and sheep⁶.

These observations raise mechanistic questions about the observed, tissue dependent, iron isotope fractionation. Mass-dependent stable isotope fractionation may occur during transport of ions or molecules, or during formation or breaking of chemical bonds. Nevertheless, isotope fractionation will only become detectable if the atomic species, differing in their isotope ratios, are separated in physically distinct compartments. Following these considerations it has been suggested that the uptake of dissolved iron via the intestinal mucosa is the most likely site of

fractionation. In the case of intestinal iron absorption, the transfer from the luminal side to the blood plasma is incomplete; on average only 1 mg of a dietary supply of approx. 10 to 15 mg ingested iron is absorbed^{1, 7}. In addition, the uptake of elemental iron requires the reduction of dietary Fe(III) to Fe(II) that is transported by a divalent metal transporter (DMT-1) via an intestinal ferric reductase (Dcytb)⁸. Redox processes involve an equilibrium isotope fractionation shifting the $^{56}\text{Fe}/^{54}\text{Fe}$ ratio by approx. 3‰ to low values in the ferrous iron as shown by experimental determination⁹ and *ab-initio* calculation of isotope fractionation factors¹⁰. Within the intestinal mucosa, a similar, oxidative process via the ferrioxidasin hephaestin is required to convert the absorbed Fe(II) back to Fe(III) for further distribution via transferrin⁸.

In this regard, the protein transferrin, bearing two iron binding sites, and contained mostly in blood plasma, is a key player¹¹. After intestinal uptake, freshly absorbed iron is loaded onto transferrin and transported within the blood plasma to various organs and tissues. Although only about 0.1% of total body iron (3 mg) is bound to transferrin, the daily turnover is significant, where 20 to 25 mg are transported through the blood plasma each day^{7a}. Most iron is transported into the red bone marrow for hemoglobin and erythrocyte synthesis. As noted previously, the internal distribution of iron within the human body is subject to

1 further isotopic fractionation^{1,5}. One possible explanation for the
2 different isotopic composition of these iron storage compartments
3 is isotope fractionation during transport or during iron loading
4 and unloading from transferrin. The same holds for iron release
5 from transferrin. Upon binding to the transferrin receptor, the
6 transferrin-receptor complex is internalized via endocytosis.
7 Should isotope fractionation during transferrin loading and
8 release be zero, then the iron composition of erythrocytes should
9 resemble that of plasma. However, transferrin also transports a
10 substantial amount of iron from other storage compartments like
11 the liver. Thus, another potential process entailing fractionation is
12 during iron storage and release from various tissue depots. Iron is
13 stored as a stable ferrihydrate complex in ferritin where Fe(II) is
14 oxidized to Fe(III) by ferrioxidase in the ferritin complex¹². It has
15 been shown in humans that the liver contains iron of which the
16 ⁵⁶Fe/⁵⁴Fe ratio is higher than that of erythrocytes^{1,5}. If during
17 release from the liver this heavy iron is not fractionated towards
18 the erythrocytes' ratio, then transferrin should contain iron
19 comprising a mixture of that delivered during hemoglobin
20 synthesis with that delivered from the liver. Hence, the
21 transferrin's isotope composition should lie between that of the
22 liver and that of erythrocytes. To date, only one study reported
23 the iron composition of human blood plasma and found it to be
24 enriched in ⁵⁶Fe over ⁵⁴Fe relative to blood, and hence being of a
25 composition closer to liver iron¹³.

26 In this study we test these hypotheses by presenting precise iron
27 stable isotope ratios measured in human erythrocytes and plasma
28 samples. Blood was sampled over a period of 21 days from 12
29 healthy male adults. The study was performed within the context
30 of a ferrokinetics and uptake study of iron following
31 administration of oral doses of the compound SBR759, labeled
32 with the stable isotope ⁵⁸Fe. The results of the iron uptake study
33 are presented in a companion paper¹⁴. A challenge for such an
34 investigation is the determination of accurate, stable iron isotope
35 ratios in plasma. Plasma iron concentrations are approx. 0.4 to 2
36 ppm compared to that of erythrocytes which can be greater than
37 400 ppm. Hence, a large organic matrix has to be separated prior
38 to mass-spectrometric analysis to avoid spectroscopic
39 interferences and shifts in the mass-bias introduced during
40 measurements by impurities contained in the samples¹⁵.
41 Presenting suitable analytical protocols is therefore a first aim of
42 this study.

43 Subjects and study design

44
45 Our investigation is part of an open-label study that was
46 undertaken to determine the ferrokinetics and uptake of iron in
47 healthy volunteers following administration of oral doses of
48 SBR759, an investigational drug being developed for the
49 treatment of hyperphosphatemia in patients with chronic kidney
50 disease, labeled with stable ⁵⁸Fe isotope, (for additional
51 information see¹⁴). The clinical part of the study was performed
52 at Covance Clinical Research Unit AG (former Swiss Pharma
53 Contract Ltd.), Allschwil, Switzerland. This study was approved
54 by the local Ethics Committee and was conducted in accordance
55 with the declaration of Helsinki (1964 and subsequent revisions)
56 and International Conference on Harmonization-Good Clinical
57 Practice guidelines. All subjects gave written informed consent

before participating in the study.

60 **Subjects:** A total of 12, iron replete (*i.e.*, nonanemic), healthy,
nonsmoking, male volunteers between 18 and 45 years of age
were recruited. This subject population was selected as their
propensity for iron absorption, noting similarities in absorption of
therapeutic iron salts by patients with chronic kidney disease
65 (CKD) on hemodialysis. Subjects with *i*) hematocrit <41%, *ii*)
hemoglobin <13.8 or >17.2 g/dL, *iii*) serum ferritin <20 or >320
ng/mL, *iv*) transferrin saturation <20%, *v*) reticulocyte count
>1.5% or platelets <100,000/ μ L, *vi*) history of anemia,
hemochromatosis or other dyscrasia(s), *e.g.* thalassemia,
70 myelodysplastic syndrome, *etc.*, were excluded from the study.
The mean age was 34.2 ± 8.8 years, the mean height was $177 \pm$
7.0 cm, the mean body weight was 80.1 ± 15.1 kg, and the mean
body mass index (BMI) was 25.3 ± 3.8 kg/m². Each subject
participated in a 21-day screening period (Day -2 to Day -21), a
75 baseline period (Day -1), and a 12 hour dosing period (Day 1,
three administrations of 4 g of [⁵⁸Fe]SBR759 each) followed by 3
weeks ambulatory period and a study completion on Day 21.
Subjects received a total daily dose of 12 g (divided in 3×4 g)
(mean \pm SD, n=12: 12.47 ± 0.017 g) of [⁵⁸Fe]SBR759.

80 Sample collection:

Serial blood samples were collected at 0 h (pre-dose; baseline), 6,
12, 16, 22 (Day 1), 26, 34 (Day 2), 106 (Day 5), 250 (Day 11),
322 (Day 14), and 490 h (Day 21) post first dose. In order to
85 avoid hemolysis during Day 1 and Day 2 when several blood
withdrawals took place, blood samples were collected by
inserting a plastic cannula fixed at the forearm. For blood
sampling at Days 5, 11, 14 and 21 a metallic needle
(venipuncture) was used for individual samplings. Blood was
90 collected into special 7.5 mL blood collection tubes for metal
analysis by slow aspiration. The tubes, which resemble a single
use syringe, contained a small and specified amount of metal
impurities (< 50 ng iron/tube; S-Monovette[®] for metal analysis;
model# 01.1604.400, Sarstedt, Germany). These tubes also
95 contained about 4-7 μ L of a lithium heparin solution
corresponding to about 0.1% of the final blood sample volume.
After blood collection the tubes were inverted gently to mix the
contents. Immediately after collection, five aliquots of whole
blood were exactly weighed into pre-labeled polypropylene
100 cryotubes and stored at $\leq -20^\circ\text{C}$.

Plasma was obtained from heparinized blood by centrifugation at
2000 \times g, at 4°C for 10 min. Plasma was recovered into pre-
weighed tubes (Monovettes for metal analysis, Sarstedt) and
stored at $\leq -20^\circ\text{C}$. Plasma samples which displayed visible signs
105 of hemolysis were excluded from data analysis. Plasma was
prepared from blood at 0 h (pre-dose), 6, 12, 16, 22 and 26 h post
first dose.

After sample collection, erythrocyte and plasma samples were
frozen immediately and stored at $\leq -20^\circ\text{C}$ until and after analysis
110 in the analytical laboratories. Samples were shipped to analytical
laboratories under dry ice to keep them frozen.

Materials and Methods

Iron stable isotope measurements by MC-ICP-MS require
separation of pure iron from the samples' matrix. The separation

1 techniques used as well as the mass-spectrometric analysis have
2 been described in detail¹⁵ and are not repeated here. However, the
3 decomposition of blood and plasma samples requires microwave-
4 aided treatment. The required protocols not described in¹⁵ are
5 reported here in more detail.

6
7 **Microwave treatment – blood samples:** After thawing, each
8 blood sample was shaken gently to ensure homogeneity. A
9 volume of *approx.* 100 μL was pipetted into pre-weighed
10 microwave treatment vessels. After adding 5 mL of 5 M HNO_3
11 and 1 mL H_2O_2 (30% w/w), microwave treatment was performed
12 on a CEM Mars 5 microwave system (CEM GmbH, Kamp-
13 Lintfort, Germany) at 1200 Watts, at 200°C for 2 hours. Only
14 after complete sample processing the resulting clear solutions
15 were transferred into Savillex[®] Teflon beakers and evaporated to
16 dryness. The residues were re-dissolved in 3 mL of 6 M
17 hydrochloric acid and split gravimetrically into two aliquots. One
18 of these aliquots was used for determining the total iron content
19 in the whole blood sample by using a calibrated inductively-
20 coupled optical emission spectroscopy (ICP-OES) system (Varian
21 Vista PRO CCD Simultaneous at the Institute for Mineralogy
22 from the Leibniz University Hannover, Germany). In addition,
23 major elements such as nickel that potentially interferes with the
24 MC-ICP-MS measurements were quantified with ICP-OES.

25
26 **Microwave treatment – plasma samples:** As plasma sample
27 amounts (*approx.* 15 mL) were too large to be decomposed in a
28 single microwave treatment vessel, each sample was split into 2
29 aliquots. To each of these 6 mL of 15 M HNO_3 and, with a lag
30 time of 10 min, 1 mL of H_2O_2 (30% w/w) was added. The
31 solutions were treated with the microwave system (heating up to
32 200°C for 25 min; 200°C was kept for 50 min). After cooling
33 down for 40 min, samples were transferred into 90 mL Savillex
34 beakers. The samples were dried and re-dissolved in 5 mL of 6 M
35 hydrochloric acid. At this stage an insoluble solid residue
36 precipitated. the residual solid phase was removed by
37 centrifugation.

38 To test whether the insoluble residues were free of iron, a
39 standard addition experiment was conducted on a plasma test
40 sample. This sample was split into two aliquots before freeze-
41 drying. The first aliquot was then split into 6 sub-splits. To each
42 of these a known amount of CertiPUR[®] iron standard was added
43 in increasing volumes. To the first aliquot, the additions were
44 made before freeze-drying. To the second aliquot, the additions
45 were made after dissolution and separation of the insoluble
46 residue by centrifugation. The iron amounts found in both
47 experiments were roughly identical within analytical error, which
48 ranged from 1 to 7%. Hence no iron from the original plasma or
49 from the additions was lost into the precipitate. Given that this
50 step did not result in loss of iron, all plasma concentration
51 measurements were performed on a 300 μL aliquot taken from
52 the 6 M hydrochloric acid solution.

53 **Iron separation:** Sample aliquots, re-dissolved in 6M
54 hydrochloric acid, were loaded onto an ion exchange column
55 containing 1 mL Dowex AG 1x8, 200-400 mesh anion exchange
56 resin (Dow Water and Process Solutions). The amount of iron
57 loaded onto the Eichrom polypropylene columns (Eichrom

Europe Laboratories, Bruz, France) was precisely determined by
60 ICP-OES so that the columns exchange capacity was not
exceeded. Iron was separated from the bulk of the matrix
following¹⁵.

61 For samples containing high initial amounts of transition metals
or organic matrices, iron separated by anion exchange
62 chromatography may not be entirely matrix-free and require
further purification. Therefore, all samples were neutralised with
ammonia and subjected to a precipitation step¹⁵. For plasma
samples which in general contain much less iron when compared
to blood, a normal precipitation step¹⁵⁻¹⁶ could not be applied.
63 Instead, plasma samples were co-precipitated after
chromatographic separation by adding 1 mL of a 1000 ppm
aluminum solution in 0.3 M HNO_3 , which was first pre-cleaned
with anion exchange chromatography to remove traces of iron.
64 The co-precipitation was achieved by adding NH_4OH to the
65 samples. To achieve maximum iron yields, the solutions were
allowed to equilibrate for 1 hour before centrifugation. The
supernatants were removed and the precipitates were washed 2-
times with Milli-Q H_2O , followed again by centrifugation and
finally re-dissolved in 1 mL 6 M hydrochloric acid. To remove
66 the aluminum, a second anion exchange chromatography was
67 necessary, which followed the same procedure as the first one at
the beginning of the iron separation scheme. The eluents were
then dried and dissolved in 5 mL 0.3 of M HNO_3 .

68 **MC-ICP-MS:** Several analytical protocols for the precise
69 determination of iron stable isotopes are published¹⁵⁻¹⁷. In this
study we follow here the method described in¹⁵ with adaptations.
Isotope ratios were determined on a Thermo Finnigan “Neptune”
Multicollector ICP-MS at the Institute for Mineralogy from the
70 Leibniz University Hannover, Germany¹⁸. Sample solutions were
nebulised and introduced by the Thermo Finnigan stable
introduction system (SIS). This system consists of a combined
cyclonic and Scott-type spray chamber. Baseline measurements
prior to each analyses were performed by taking a deflected
71 baseline at the start of a sequence. An “on-peak zero”
measurement was done before each sample and standard
measurement on 0.3 M HNO_3 to subtract a background signal
introduced by interaction of the sample and the ion beam with
parts of the inlet system and the mass spectrometer from
72 measured standard and sample signals.

73 Whereas argides can be resolved from each corresponding iron
isotope due to the high mass resolving power of the MC-ICP-MS,
potential isobaric interferences of $^{54}\text{Cr}^+$ and $^{58}\text{Ni}^+$ on $^{54}\text{Fe}^+$ and
 $^{58}\text{Fe}^+$, respectively, were minimised by removal of chromium and
74 nickel using anion exchange chromatography. The purity of the
fractions after anion exchange chromatography was monitored by
ICP-OES. To correct for minor residual interferences, the
isotopes ^{52}Cr and ^{60}Ni were measured in parallel with ^{54}Fe , ^{56}Fe ,
 ^{57}Fe and ^{58}Fe . The interference correction of ^{54}Cr on ^{54}Fe and ^{58}Ni
75 on ^{58}Fe was performed according to¹⁵. Briefly, the amount of ^{54}Cr
was calculated from the ^{52}Cr intensity measured simultaneously
and from the average natural $^{54}\text{Cr}/^{52}\text{Cr}$ ratio. The amount of
interfering ^{58}Ni was calculated from the average natural $^{60}\text{Ni}/^{58}\text{Ni}$
ratio. An instrumental mass discrimination factor was applied to
76 ^{52}Cr and ^{58}Ni intensities, respectively, which was determined
from the measured $^{57}\text{Fe}/^{56}\text{Fe}$ ratio by applying an exponential

mass bias law.

Instrumental mass discrimination induced by incomplete removal of the sample matrix or non-reproducible mass-spectrometric run conditions potentially introduced a substantial bias into the resulting isotope ratio measurements. As iron concentrations in blood plasma are low, and a large organic matrix is present, these measurements are particularly prone to such bias. For this reason the measurement of 18 separated plasma iron samples was repeated on a similar instrument (Thermo Neptune Plus Multicollector ICP-MS) based at the GeoForschungsZentrum Potsdam. For these measurements an ESI Apex-Q desolvating apparatus using a low flow (aspiration rate of 100 $\mu\text{L min}^{-1}$) PFA self-aspirating nebuliser was used. The ESI Apex-Q apparatus consists of a heated cyclonic glass spray chamber coupled with a Peltier element-cooled glass spiral condenser. The mass spectrometer's interface was equipped with Thermo "Jet" cones. This instrumental setup, that differs considerably from that used at the instrument at the University of Hannover, would detect a potential matrix-induced mass bias in the form of non-reproducible isotope ratios.

Iron standards for controlling MC-ICP-MS measurements:

Commercially available "IRMM-014" iron bracketing reference standard was used (from EU Institute for Reference Materials and Measurements, Geel, Belgium)¹⁹. Additionally, the "JM" internal iron laboratory standard (Fe Puratronic wire, 99.998% purity, lot NM36883; Johnson & Matthey, London, UK) was used for optimizing instrumental run conditions and assessing instrumental reproducibility. Differences in Fe isotope composition between "JM" and "IRMM-014" Fe solutions have been reported^{15, 18}. In this study, additionally a second internal laboratory standard "HanFe" was measured against the "IRMM-014" iron standard. Iron isotope data of samples is only accepted if the iron isotope composition of a known iron standard measured repeatedly in the same analysis session is within the uncertainty limits¹⁵. To ensure this in each session, three to six samples of the internal "JM" and new internal "HanFe" iron reference standards were measured in most sessions. For the "JM" reference, the mean values obtained in 96 measurements over 18 sessions agreed with those given in¹⁵ and "HanFe" yielded $\delta^{56}\text{Fe}/^{54}\text{Fe}$ values within the range of 0.28 to 0.30‰ as now measured by four different laboratories²⁰ (Supplementary Table S1).

Iron isotope fractionation due to incomplete recovery.

Quantitative recovery and removal of matrix elements during iron separation and precipitation was controlled by iron concentration measurements with small aliquots of the samples before and after each step by ICP-OES. This check is important because non-quantitative recovery could result in artificial isotope fractionation²¹. A 90% recovery limit for iron recovery after ion exchange separation was set as acceptance criterion. The total iron recovery was monitored by ICP-OES analysis. Only in four blood samples the iron recovery was lower than 90%. One sample was partially lost and did not allow calculating the iron recovery. Only in two plasma samples, the iron recovery was lower than 90%. One sample was partially lost and could not be analyzed. The total procedural iron blanks were measured with

mostly less than 60 ng. This was less than 1% of the processed iron (with a minimum measurable Fe content of 6 μg) and was considered to be insignificant.

Isotope ratio reporting. All isotope ratios were reported in permil deviations from the "IRMM-014" reference material:

$$\frac{\delta^{56}\text{Fe}}{\text{‰}} = \left(\frac{{}^{56}\text{Fe}/{}^{54}\text{Fe}_{\text{Sample}}}{{}^{56}\text{Fe}/{}^{54}\text{Fe}_{\text{IRMM-014}}} - 1 \right) * 1000$$

A similar equation is used for $\delta^{57}\text{Fe}$ and $\delta^{58}\text{Fe}$ when ${}^{56}\text{Fe}$ is replaced by ${}^{57}\text{Fe}$ or ${}^{58}\text{Fe}$, respectively.

Results

MC-ICP-MS Method validation and assessment

Iron isotope specificity and isobaric interferences: To avoid artefacts introduced by a high chromium or nickel corrections, Fe isotope analyses with ${}^{54}\text{Cr}/{}^{54}\text{Fe} > 0.1\text{‰}$ shall be rejected from the data set as well as $\delta^{58}\text{Fe}$ values of samples with ${}^{58}\text{Ni}/{}^{58}\text{Fe} > 10\text{‰}$ ¹⁵. The interferences on ${}^{58}\text{Fe}$ are reported in some detail here as they are important for the companion paper¹⁴. In this study, the ${}^{54}\text{Cr}/{}^{54}\text{Fe}$ ratios in blood ranged from 0.0018‰ to 0.029‰ and the ${}^{58}\text{Ni}/{}^{58}\text{Fe}$ ratios ranged from zero to 6.20‰. The ${}^{54}\text{Cr}/{}^{54}\text{Fe}$ ratios in plasma ranged from 0.022‰ to 0.128‰ and the ${}^{58}\text{Ni}/{}^{58}\text{Fe}$ ratios ranged from zero to 9.09‰. Two blood samples displayed high ${}^{58}\text{Ni}/{}^{58}\text{Fe}$ ratios of 18.1‰, 34.7‰, and one plasma sample a ${}^{58}\text{Ni}/{}^{58}\text{Fe}$ ratio of 12.9‰, respectively. Since their measured $\delta^{58}\text{Fe}$ values were sufficiently high after absorption of SBR759, these samples were therefore nonetheless included in the iron absorption calculation¹⁴.

Another test for the presence of isobaric interferences is the use of three isotope plots, where offsets from the predicted mass-dependent fractionation curve indicate the presence of isobaric interferences. The $\delta^{57}\text{Fe}/\delta^{56}\text{Fe}$ graphs of normalised iron isotope ratios ($\delta^{57}\text{Fe}/{}^{54}\text{Fe}$ versus $\delta^{56}\text{Fe}/{}^{54}\text{Fe}$ and $\delta^{58}\text{Fe}/{}^{54}\text{Fe}$ versus $\delta^{56}\text{Fe}/{}^{54}\text{Fe}$) of the "JM" and "HanFe" iron standards are depicted in Figure S1 a-d and of baseline blood and plasma samples in Figure S1 e-h. (Supplementary information). All standard and sample results plot onto the mass-dependent isotope fractionation line, which indicates measurements that were free of spectral interferences. Blood and plasma samples post first dose containing absorbed [${}^{58}\text{Fe}$]SBR759-related iron might contain a relatively higher fraction of ${}^{57}\text{Fe}$ (i.e. "impurity" in the ${}^{58}\text{Fe}$ label), as compared to its natural abundance. The isotopic composition of [${}^{58}\text{Fe}$]SBR759 relative to the international "IRMM-014" reference material was determined to be 5.706% ${}^{54}\text{Fe}$, 89.552% ${}^{56}\text{Fe}$, 2.077% ${}^{57}\text{Fe}$, and 2.665% ${}^{58}\text{Fe}$ ¹⁴, which compares to 5.845% ${}^{54}\text{Fe}$, 91.754% ${}^{56}\text{Fe}$, 2.12% ${}^{57}\text{Fe}$, and 0.281% ${}^{58}\text{Fe}$ for the reference material "IRMM-014"¹⁹. Hence in this study $\delta^{57}\text{Fe}$ and $\delta^{58}\text{Fe}$ for post first dose samples are not used.

For plasma samples, we observed higher ${}^{52}\text{Cr}$ levels than for either blood samples or the standard materials. We tested whether this increase was due to unresolved ${}^{40}\text{Ar}/{}^{12}\text{C}$ interferences on mass 52. In that case the ${}^{54}\text{Fe}$ intensities would be over-corrected for

^{54}Cr . We plotted the $\delta^{57}\text{Fe}/^{56}\text{Fe}$ ratio against $\delta^{56}\text{Fe}/^{54}\text{Fe}$ of plasma baseline samples (Fig. 1). The $^{57}\text{Fe}/^{56}\text{Fe}$ ratio is not subject to a Cr interference correction. The fact that all data plot on the mass-dependent fractionation curve, regardless of whether they have been corrected for Cr interferences, shows that Cr corrections did not introduce a bias resulting from excessive ^{54}Fe corrections.

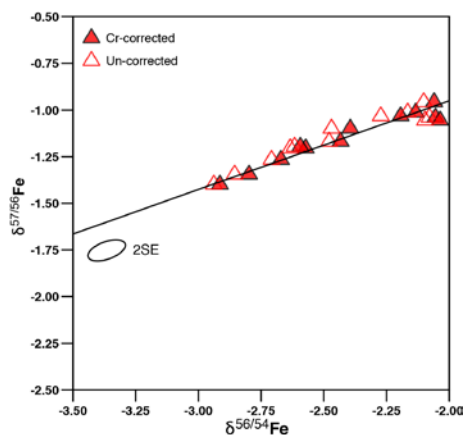


Figure 1: $\delta^{57}\text{Fe}/^{56}\text{Fe}$ versus $\delta^{56}\text{Fe}/^{54}\text{Fe}$ diagram as test for excessive ^{54}Cr interference due to presence of a $^{40}\text{Ar}^{12}\text{C}$ interference on the monitor isotope ^{52}Cr in plasma baseline samples (taken before administration of SBR759 to ensure absence of a ^{57}Fe contribution from the spike). The $^{57}\text{Fe}/^{56}\text{Fe}$ ratio is not subject to a Cr interference correction. Open symbols: $\delta^{56}\text{Fe}$ not corrected for “Cr” interference; closed symbols: $\delta^{56}\text{Fe}$ ratios corrected for interferences. The error ellipse denotes the correlated 2-standard deviation as derived from “JM” standard measurements (Supplementary table S1). The fact that all data plots on the mass-dependent fractionation curve shows that Cr corrections did not introduce a bias resulting from excessive ^{54}Fe corrections.

Instrumental iron isotope mass bias drift: The blood and plasma samples were also monitored for their instrumental mass bias drift during measurements. Samples for which the two directly bracketing standard measurements exceed an instrumental mass bias drift of ± 200 ppm on the $^{56}\text{Fe}/^{54}\text{Fe}$ ratio were set as rejection criterion¹⁵. As plasma samples were difficult to measure due to their complex matrix, we relaxed this criterion slightly to 220 ppm. The mass bias drift for blood samples ranged between -202 ppm to 162 ppm (mean \pm SD of the absolute values: 44.9 ± 30.0 ppm (n=181)). Only one sample exceeded this bias shift slightly (202 ppm) and was rejected. The drift in mass bias on the $^{56}\text{Fe}/^{54}\text{Fe}$ ratios measured in plasma samples ranged from -476 ppm to 321 ppm (mean \pm SD of the absolute values: 96.8 ± 96.6 ppm, n=71).

Long term iron concentration and isotope ratio stability of blood and plasma samples

Mean subjects' iron concentrations in erythrocytes (as measured in whole blood samples) ranged between 428 and 497 ppm (Table 1); mean plasma iron concentrations varied between 0.59 and 1.2 ppm (Table 1). Iron concentrations in erythrocytes samples taken from individual subjects at different intervals varied by ± 17 to ± 38 ppm (2-SD over all samples, Supplementary Table S2). Plasma samples varied by ± 0.25 to ± 1.2 ppm (2-SD over all

samples, Table 1, Supplementary Table S3) in their iron concentrations. This means that relative variations in plasma iron concentrations were much larger than those in erythrocytes.

$\delta^{56}\text{Fe}$ in erythrocytes ranges from *approx.* -3.1 to -2.2‰ (Figure 2), a range typical for male Caucasian adults³. The 2-SD value of erythrocytes samples taken at different intervals from an individual subject varied between ± 0.06 and ± 0.15 ‰ (2-SD),

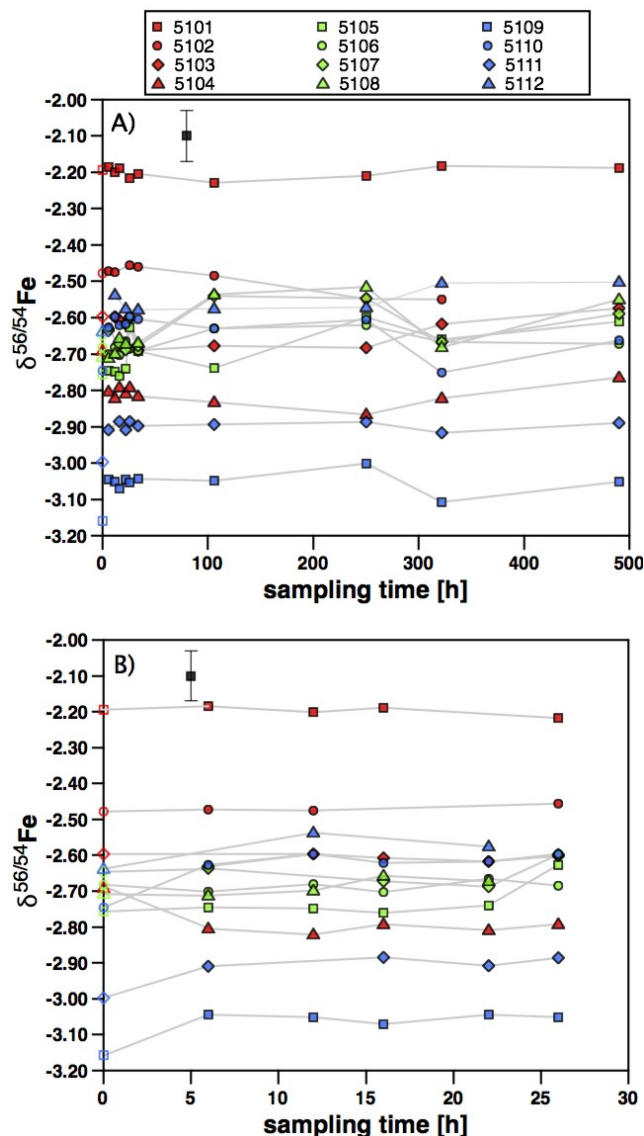


Figure 2: $\delta^{56}\text{Fe}$ in erythrocytes of the 12 subjects against sampling time. A) All data from Day 1 to Day 21. Note that $\delta^{56}\text{Fe}$ in erythrocytes is invariant with time over this period. B) The first 26 hours were sampled at higher time resolution. The symbols denote individual subjects.

which is in most cases indistinguishable from the analytical precision of laboratory standards (Table 1). Hence, erythrocytes Fe isotopic compositions can be regarded as uniform over the 21 days investigated (Fig. 2). In plasma samples, $\delta^{56}\text{Fe}$ values ranged from *approx.* -3.0 to -2.0‰ (Fig. 3). The 2-SD value of all plasma samples from an individual subject was mostly around

$\pm 0.2\%$, but varied between ± 0.09 and $\pm 0.49\%$ (2-SD, Table 1). We quantified the attainable reproducibility for plasma measurements from our inter-laboratory comparison, which provides the strongest possible quantification of the most likely source of uncertainty, i.e. mass-spectrometric bias from

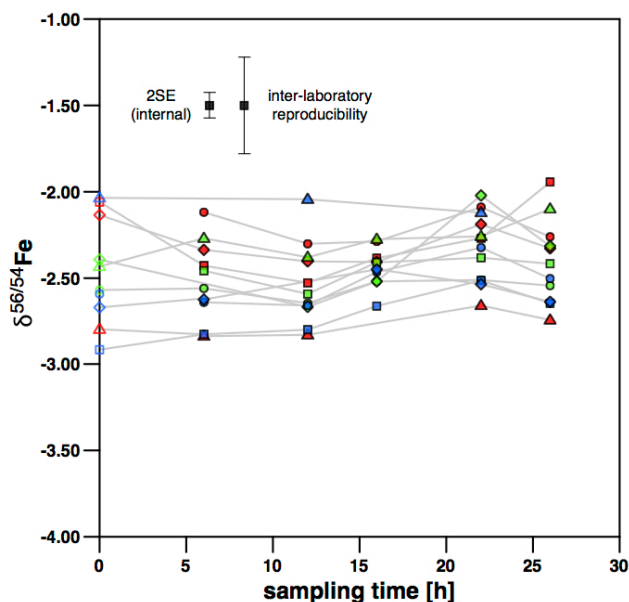


Figure 3: $\delta^{56}\text{Fe}$ in plasma of the 12 subjects against sampling time. The symbols denote individual subjects and are the same as in Fig. 2. Error bars show 2 standard deviations.

uncorrectable matrix effects. For our 16 duplicate measurements $\delta^{56}\text{Fe}$ is on average 0.26% and $\delta^{57}\text{Fe}$ 0.37% lower at GFZ Potsdam than at the University of Hannover (Supplementary Table S3). This systematic bias resulted from the entirely different run conditions and places a lower limit on the reproducibility that is attainable for such complex matrix. Such an effect might arise for example from excess amounts of organic carbon that were still present in the Fe separates during MC-ICP-MS analysis. Calculating the 2-SD value from the sixteen duplicates, we obtain for $\delta^{56}\text{Fe}$ 0.28% and for $\delta^{57}\text{Fe}$ 0.39% . This reproducibility we use in the interpretation of the data. The plasma samples taken at 26 hours of subjects 5101 and 5102, respectively, yielded $\delta^{56}\text{Fe}$ values that deviated more than 25% from that of all other plasma samples of these subjects (Supplementary Table S3). We have no explanation for this deviation, and used instead the repeat measurement performed at GFZ Potsdam that agreed well with the other samples from these subjects. Overall, the iron isotopic composition in plasma was more variable than in erythrocytes. We attribute this variability to the lower reproducibility of these measurements.

$\delta^{56}\text{Fe}$ in plasma samples is higher than that in erythrocytes in 11 out of 12 samples by 0.01 to 0.51% (Fig. 4). Only subject 5101 features a $\delta^{56}\text{Fe}$ value in its plasma sample that is lower than that in erythrocytes by 0.21% . The average difference in $\delta^{56}\text{Fe}$ between plasma iron and erythrocytes iron is 0.23% (Table 1). This difference is only marginally in excess of the 2-SD value resulting from our inter-laboratory comparison. We therefore cannot conclude with certainty that the difference is

real. We note that after administration of $[\text{}^{58}\text{Fe}]\text{SBR759}$, ^{57}Fe in plasma samples is elevated over baseline as the ^{58}Fe spike added also contains elevated levels of ^{57}Fe (see supplementary Table S4). ^{56}Fe however is unaffected, and plots of $^{56}\text{Fe}/^{54}\text{Fe}$ vs. $^{58}\text{Fe}/^{54}\text{Fe}$ do not yield correlations as would be expected if contamination of ^{56}Fe by $[\text{}^{58}\text{Fe}]\text{SBR759}$ would occur. However, plasma samples might have been affected by hemolysis. We proceed to discuss this question in comparison to literature data in the next section.

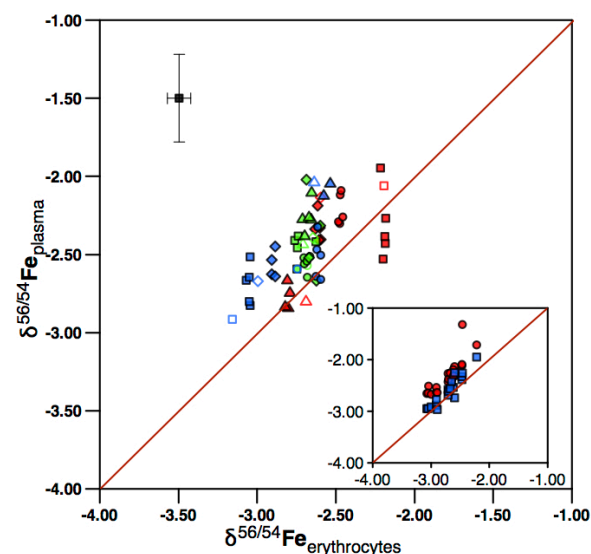


Figure 4: $\delta^{56}\text{Fe}$ in plasma against erythrocytes. Most data plot within 0.5% within the 1:1 line, showing that the individual subjects carry a distinct iron isotope composition that is similar between erythrocytes and plasma. The symbols denote individual subjects and are the same as in Fig. 2. The inset shows results of the inter-laboratory comparison of plasma samples. Samples measured at Hannover are shown in red, samples at GFZ Potsdam in blue. The plasma samples taken at 24 hours of subjects 5101 and 5102, respectively, yielded $\delta^{56}\text{Fe}$ that deviated significantly from that of all other plasma samples of these subjects when measured at Hannover. For these samples the Potsdam data were plotted in the main plot.

Discussion

Lysis of erythrocytes with liberation of hemoglobin (hemolysis) may occur *in vitro* when blood samples are taken and plasma is prepared. Hemolysis can further occur if the centrifugation procedure has failed to result in complete separation between iron in erythrocytes and iron in plasma. Given the large concentration differences (480 ppm versus $\sim 1\text{ ppm}$, respectively) minor hemolysis could contaminate plasma samples with erythrocyte isotope composition. In order to minimize hemolysis during several consecutive blood withdrawals, blood samples were collected via a plastic cannula placed in a forearm vein that remained through sampling 26 hours post last dose. Blood sampling and plasma preparation was carried out throughout the study by qualified clinical and laboratory personnel. Study specific training on blood sampling, including the recognition and

minimization of hemolysis, was also provided.

As spectrophotometric measurements of hemoglobin levels in our plasma samples were not done, we evaluate this possibility based on literature data. Our measured plasma iron concentrations are within known values that range between 0.75 and 1.75 ppm for males^{4b, 22} suggesting that iron in plasma was not contaminated by erythrocyte iron. We can evaluate the contribution of iron to plasma from hemoglobin further from hemoglobin levels quantified in plasma by spectrophotometry²³. The hemoglobin levels in plasma reported in that study range between 0.002 and 0.019 (mean 0.007) w/V%. Using the iron concentration of hemoglobin (0.35 weight%) typical iron contamination levels between 0.07 and 0.66 ppm with a mean of 0.24 ppm can be calculated. Since our samples have been taken and centrifuged with great care, we adopt the mean minimum hemoglobin iron contamination level of 0.24 ppm and assume that all iron in excess of this value is truly plasma iron. This assumption means that iron concentrations of uncontaminated plasma are between 0.5 and 1.5 ppm.

To calculate the plasma iron isotope composition despite the possibility of contamination by erythrocyte hemolysis, we plotted the difference in $\delta^{56}\text{Fe}$ between erythrocytes and plasma against the inverse concentration of iron in plasma (Fig. 5) In such a diagram, mixtures yield linear relationships and the end member compositions can be inferred. The figure shows that the isotope difference between Fe in erythrocytes and Fe in plasma increases with decreasing concentration. As $\delta^{56}\text{Fe}_{\text{erythrocytes}}$ is constant for each subject this means that $\delta^{56}\text{Fe}_{\text{plasma}}$ increases with decreasing concentration. This trend is more pronounced for samples taken from Hours 22 to 26 (open colored symbols) than for those taken from Hours 0 to 16 (closed colored symbols). We explain this trend with the decreasing effect of hemolysis introduced during sampling, as the inserted plastic cannula remained in place throughout. Hence the samples taken last approach the true $\delta^{56}\text{Fe}_{\text{plasma}}$ most closely.

A linear regression analysis through all our data (Fig. 5) yields a slope of -0.2 with R^2 of 0.2. We used this slope to model where $\delta^{56}\text{Fe}_{\text{erythrocytes}} - \delta^{56}\text{Fe}_{\text{plasma}}$ would plot if plasma were contaminated by variable amounts of erythrocytes during centrifugation (Fig. 5). In this calculation, we assumed the “pure”, but unknown plasma iron isotope composition with three independent models, as shown by the lines and tick marks in Fig. 5: in each model the iron concentration in erythrocytes was set at 480 ppm, while the iron concentration in uncontaminated plasma was set to 0.4 ppm. For our data the isotope difference $\Delta^{56}\text{Fe}_{\text{erythrocytes-plasma}}$ obtained to satisfy a slope of -0.2 is -0.4‰. We conclude that this value is the average difference between erythrocyte Fe isotope composition and uncontaminated plasma isotope composition in our samples.

We can compare this relationship to the one obtained by Albarède et al.¹³. Fe in these serum samples¹³ were on average 1‰ heavier than erythrocytes in females and 0.6‰ heavier in males, respectively. We note however that while our mean Fe concentrations in plasma (0.8 ppm) were similar to the serum data of van Heghe et al.^{4b} (0.9 ppm), Fe concentrations in serum

samples of Albarède et al.¹³ were higher with a mean concentration of 1.4 ppm. If the samples in that study were still affected by hemolysis, modeled slopes demand that their $\delta^{56}\text{Fe}$ in the serum differs by -1.5‰ from than erythrocytes in males, and by -2.5‰ in females, respectively (see $\Delta^{56}\text{Fe}$ erythrocytes–plasma models -1.5‰ and -2.5‰ in Fig. 5). Such strong isotope fractionation we regard as unlikely. If these experiments were not affected by hemolysis, the possibility remains that isotope ratios are subject to an unidentified analytical mass bias. Given the difficult matrix that plasma or serum represents, and the challenge we have encountered in developing a suitable analytical protocol, this explanation cannot be fully excluded.

Using our new plasma data presented here, we proceed with the conclusion that $\delta^{56}\text{Fe}$ in plasma is at least 0.4‰ higher than that in erythrocytes.

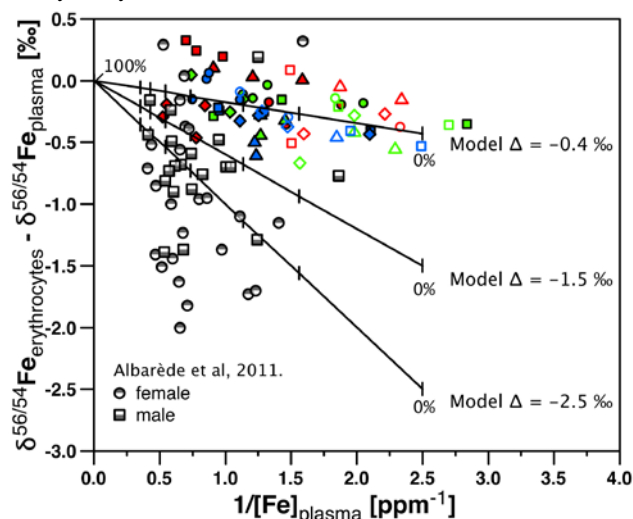


Figure 5: $\delta^{56}\text{Fe}_{\text{erythrocytes}} - \delta^{56}\text{Fe}_{\text{plasma}}$ versus $1/[\text{Fe}]_{\text{plasma}}$ concentration in plasma. The colored symbols are from this study (subjects as in Fig. 2), where closed symbols show data of samples taken from 0 to 16 hours and open symbols samples taken from 22 to 26 hours. The grey symbols from Albarède et al.¹³. The lines and tick marks show three mixing models that serve to predict how data would be aligned if plasma iron were contaminated by erythrocyte-sourced iron. In each model the iron concentration in erythrocytes was set to 480 ppm, while the iron concentration in plasma was set to 0.4 ppm. The true isotope difference $\Delta^{56}\text{Fe}$ erythrocytes–plasma was set to -0.4‰, -1.5‰, and -2.5‰ in the three models. The weight% tick marks on the model curve indicate the weight fraction of total erythrocytes sample mixed into total plasma by hemolysis (from 0 to 0.5 and 100 weight%).

Where does the isotope fractionation between plasma Fe and erythrocyte Fe occur? The liver, spleen, and red bone marrow contain iron that can be up to 1‰ heavier than erythrocytes^{1, 5} too. Transferrin is the molecule transporting iron contained in plasma into and from these compartments. In this regard, it is important that this study recruited healthy male subjects who were iron replete *i.e.* nonanemic and are expected to have a normal erythrocyte turnover rate. At the end of their ~120 day lifespan, heme iron from erythrocytes in blood, and myoglobin from damaged muscle tissue are recycled after being phagocytosed by circulating macrophages or the

Table 1: Mean and 2-SD of $\delta^{56/54}\text{Fe}$ iron in blood and in plasma and the difference between means in each subject

Subject	Blood Samples						Plasma Samples						Difference Plasma - Blood	
	0-490 hours			0-26 hours			0-26 hours						0-26 hours	
	Fe conc [ppm]	2-SD	$\delta^{56/54}\text{Fe}$ [‰]	2-SD	$\delta^{56/54}\text{Fe}$ [‰]	2-SD	Fe conc [ppm]	2-SD	$\delta^{56/54}\text{Fe}$ [‰]	2-SD	$\delta^{56/54}\text{Fe}$ [‰]	2-SD	$\delta^{56/54}\text{Fe}$ [‰]	
						Hannover			Potsdam			Hann	Pots	
5101	433	32	-2.214	0.059	-2.194	0.032	1.01	0.63	-2.31	0.45	-1.95	-	-0.12	0.25
5102	428	22	-2.490	0.075	-2.470	0.019	0.59	0.25	-2.21	0.20	-2.33	0.13	0.26	0.15
5103	452	38	-2.627	0.079	-2.609	0.027	1.21	1.19	-2.30	0.23	-2.40	-	0.31	0.21
5104	471	19	-2.801	0.090	-2.785	0.095	0.70	0.48	-2.77	0.15	-	-	0.01	-
5105	491	26	-2.708	0.115	-2.730	0.102	0.77	0.97	-2.45	0.17	-	-	0.28	-
5106	460	17	-2.676	0.059	-2.686	0.028	0.66	0.36	-2.56	0.10	-	-	0.13	-
5107	466	25	-2.626	0.109	-2.648	0.069	0.92	0.64	-2.38	0.49	-2.58	-	0.26	0.06
5108	443	26	-2.640	0.151	-2.690	0.048	0.66	0.31	-2.29	0.23	-2.61	0.11	0.40	0.08
5109	442	28	-3.061	0.081	-3.070	0.088	0.71	0.59	-2.73	0.29	-2.95	-	0.34	0.12
5110	495	28	-2.642	0.112	-2.634	0.112	1.02	0.48	-2.53	0.25	-	-	0.10	-
5111	497	25	-2.904	0.067	-2.910	0.090	0.71	0.30	-2.58	0.18	-2.88	0.17	0.33	0.03
5112	495	28	-2.561	0.075	-2.573	0.069	0.71	0.35	-2.07	0.09	-	-	0.51	-
mean	464		-2.663		-2.667		0.81		-2.43		-2.53		0.23	0.13
min	428	17	-3.061	0.059	-3.070	0.019	0.59	0.25	-2.77	0.09	-2.95	0.11	-0.12	0.03
max	497	38	-2.214	0.151	-2.194	0.112	1.21	1.19	-2.07	0.49	-1.95	0.17	0.51	0.25

reticuloendothelial system (RES) of the spleen²⁴ and released back into the plasma bound to transferrin. This recycling rate is approximately 2 mg per day from erythrocytes and another 2 mg from muscle tissue²⁵, potentially dominating the isotope composition of the iron contained in plasma. As heavy liver iron is stored in the ferritin molecule, release of iron from ferritin could play a key role in tissue fractionation since tissues enriched in heavier iron isotopes are generally high in ferritin content. In general, two chemical reaction types, binding to organic molecules and redox processes, lead to different degrees of isotope fractionation. Fe(III) – chelate fractionation is +0.2‰ at equilibrium²⁶. As this fractionation factor is too small to explain the large difference between plasma and liver iron or erythrocyte iron. Reduction from ferric to ferrous iron through activity of a reductase is a more likely explanation^{6,11}. Iron binding onto ferritin involves oxidation of iron *via* a ferrioxidase²⁷. As noted in the introduction, these redox processes can be accompanied with equilibrium isotope fractionation amounting to up to 3‰ in $\delta^{56}\text{Fe}$ ⁹⁻¹⁰, potentially favouring heavy iron isotopes in ferritin. If transferrin iron remains in the ferric state, whereas heme iron carried by erythrocytes is in the ferrous state¹, then plasma iron isotope composition will be intermediate between that of erythrocyte and ferritin iron, as the liver will release preferentially heavy iron isotopes, which is then mixed with light iron isotopes from quantitative erythrocyte recycling. Hence, redox processes play the decisive role in iron isotope fractionation between compartments of the human body, regardless of whether the pathways are direct or indirect^{1,13}.

Conclusions

A chemical separation procedure using microwave treatment and anion exchange chromatography was developed for analysis of iron isotopes in human blood plasma by MC-ICP-MS. The isotope composition of plasma reacts exceedingly sensitive to hemolysis which may occur during blood sampling and subsequent centrifugation. Hence, while within analytical precision the iron isotopic ratios are identical between whole blood and plasma of 12 healthy male Caucasian adults, these results are also compatible with a plasma iron isotope composition that is at least 0.4‰ higher in $\delta^{56}\text{Fe}$ than that of erythrocytes. Release and uptake of iron onto ferritin is a key player that can induce isotope fractionation, mixing isotopically heavier iron from the liver into plasma while at the same time lighter iron is released from erythrocytes. Redox processes involved in ferritin binding and unbinding are the key players.

Acknowledgements

We acknowledge Ingo Horn (Leibniz Universität Hannover, Germany), for supporting mass spectrometric measurements and Ronny Schoenberg (Universität Tübingen, Germany) for advice in the design of this study, Gerrit Budde (Universität Münster, Germany) for laboratory support, and Thomas Walczyk (National University of Singapore) and an anonymous manuscript reviewer for their constructive comments.

Notes and references

- ^a Institute for Mineralogy, Leibniz Universität Hannover, Germany
^b GFZ German Research Center for Geosciences, Potsdam, Germany (present Address) fvb@gfz-potsdam.de
^c NIBR/DMPK, Novartis Pharma AG, Basel, Switzerland

^d Institute of Geological Sciences, University of Berne, Switzerland
(present Address)

^e NIBR/Translational Medicine, Novartis Corporation, East Hanover,
USA

^f Clinical Science and Innovation, Novartis Pharma AG, Basel,
Switzerland

^g Chemical and Analytical Development, Novartis Pharma AG, Basel,
Switzerland

[†] Electronic Supplementary Information (ESI) available: [Supplement 1: Compilation of internal laboratory reference iron standards. Supplement 2: Measured Fe concentration and isotope data on blood. Supplement 2: Measured Fe concentration and isotope data on blood plasma. Supplement 4: SBR759 Measured iron isotope composition]. See DOI: 10.1039/b000000x/

References

1. T. Walczyk, F. von Blanckenburg, Deciphering the iron isotope message of the human body. *International Journal of Mass Spectrometry* 2005, 242, 117-134.
2. (a) F. Albarède, B. L. Beard, in *Geochemistry of Non-Traditional Stable Isotopes*, ed. C. M. Johnson, B. L. Beard, F. Albarède. Mineralogical Society of America: Blacksburg, 2004, vol. 55, pp 113-152; (b) N. Jakubowski, T. Prohaska, F. Vanhaecke, P. H. Roos, T. Lindemann, Inductively coupled plasma- and glow discharge plasma-sector field mass spectrometry. *Journal of Analytical Atomic Spectrometry* 2011, 26, 727-757, DOI: 10.1039/c0ja00007h.
3. T. Walczyk, F. von Blanckenburg, Natural iron isotope variations in human blood. *Science* 2002, 295, 2065-2066.
4. (a) T. Ohno, A. Shinohara, I. Kohge, M. Chiba, T. Hirata, Isotopic analysis of Fe in human red blood cells by multiple collector-ICP-mass spectrometry. *Analytical Sciences* 2004, 20, 617-621; (b) L. Van Heghe, J. Delanghe, H. Van Vlierberghe, F. Vanhaecke, The relationship between the iron isotopic composition of human whole blood and iron status parameters. *Metallomics* 2013, 5, 1503-1509, DOI: Doi 10.1039/C3mt00054k; (c) F. von Blanckenburg, J. Noordmann, M. Guelke-Stelling, The Iron Stable Isotope Fingerprint of the Human Diet. *J Agr Food Chem* 2013, 61, 11893-11899, DOI: 10.1021/jf402358n.
5. K. Hotz, H. Augsburg, T. Walczyk, Isotopic signatures of iron in body tissues as a potential biomarker for iron metabolism. *Journal of Analytical Atomic Spectrometry* 2011, 26, 1347-1353, DOI: 10.1039/c0ja00195c.
6. V. Balter, A. Lamboux, A. Zazzo, P. Telouk, Y. Leverrier, J. Marvel, A. P. Moloney, F. J. Monahan, O. Schmidt, F. Albarede, Contrasting Cu, Fe, and Zn isotopic patterns in organs and body fluids of mice and sheep, with emphasis on cellular fractionation. *Metallomics* 2013, 5, 1470-1482, DOI: Doi 10.1039/C3mt00151b.
7. (a) M. W. Hentze, M. U. Muckenthaler, N. C. Andrews, Balancing acts: Molecular control of mammalian iron metabolism. *Cell* 2004, 117, 285-297, DOI: 10.1016/s0092-8674(04)00343-5; (b) W. I. Leong, B. Loenneker, in *Iron Physiology and Pathophysiology in Humans*, ed. G. J. Anderson, G. D. MacLaren. Humana Press: New York, 2012, pp 81-99.
8. (a) N. C. Andrews, P. J. Schmidt, Iron Homeostasis. *Annual Review of Physiology* 2007, 69, 69-85; (b) A. T. McKie, R. J. Simpson, in *Iron Physiology and Pathophysiology in Humans*, ed. G. J. Anderson, G. D. MacLaren. Humana Press: New York, 2012, pp 101-116.
9. S. A. Welch, B. L. Beard, C. M. Johnson, P. S. Braterman, Kinetic and equilibrium Fe isotope fractionation between aqueous Fe(II) and Fe(III). *Geochim. Cosmochim. Acta* 2003, 67, 4231-4250.
10. A. D. Anbar, A. A. Jarzecki, T. G. Spiro, Theoretical investigation of iron isotope fractionation between Fe(H₂O)(3+)(6) and Fe(H₂O)(2+)(6) : Implications for iron stable isotope geochemistry. *Geochim. Cosmochim. Acta* 2005, 69, 825-837, DOI: 10.1016/j.gca.2004.06.012.
11. R. M. Graham, A. C. G. Chua, D. Trinder, in *Iron Physiology and Pathophysiology in Humans*, ed. G. J. Anderson, G. D. MacLaren. Humana Press: New York, 2012, pp 117-139.
12. N. D. Chasteen, P. M. Harrison, Mineralization in ferritin: an efficient means of iron storage. *Journal of structural Biology* 1999, 126, 182-194.
13. F. Albarède, P. Telouk, A. Lamboux, K. Jaouen, V. Balter, Isotopic evidence of unaccounted for Fe and Cu erythropoietic pathways. *Metallomics* 2011, 3, 926-933, DOI: 10.1039/c1mt00025j.
14. H. P. Gschwind, D. G. Schmid, F. von Blanckenburg, M. Oelze, K. van Zuilen, A. Slade, S. Stitah, D. Kaufmann, P. Swart, Iron uptake and ferrokinetics in healthy male subjects of an iron-based oral phosphate binder (SBR759) labeled with the stable isotope ⁵⁸Fe. *Metallomics* submitted.
15. R. Schoenberg, F. von Blanckenburg, An assessment of the accuracy of stable Fe isotope ratio measurements on samples with organic and inorganic matrices by high-resolution multicollector ICP-MS. *International Journal of Mass Spectrometry* 2005, 242, 257-272.
16. A. Stenberg, D. Malinovsky, I. Rodushkin, H. Andrés, C. Pontér, B. Öhlander, D. C. Baxter, Separation of Fe from whole blood matrix for precise isotopic ratio measurements by MC-ICP-MS: a comparison of different approaches. *Journal of Analytical Atomic Spectrometry* 2003, 18, 23-28.
17. N. Dauphas, A. Pourmand, F. Z. Teng, Routine isotopic analysis of iron by HR-MC-ICPMS: How precise and how accurate? *Chemical Geology* 2009, 267, 175-184, DOI: 10.1016/j.chemgeo.2008.12.011.
18. S. Weyer, J. Schwieters, High precision Fe isotope measurements with high mass resolution MC-ICPMS. *International Journal of Mass Spectrometry* 2003, 226, 355-368.
19. P. D. P. Taylor, R. Maeck, P. DeBievre, Determination of the absolute isotopic composition and atomic-weight of a reference sample of natural iron. *Int. J. Mass Spectrom. Ion Proc.* 1992, 121, 111-115 https://irmm.jrc.ec.europa.eu/refmat_pdf/IRMM-014_cert.pdf.
20. K. Moeller, R. Schoenberg, T. Grenne, I. H. Thorseth, K. Drost, R. B. Pedersen, Comparison of iron isotope variations in modern and Ordovician siliceous Fe oxyhydroxide deposits. *Geochim. Cosmochim. Acta* 2014, 126, 422-440.
21. A. D. Anbar, J. E. Roe, J. Barling, K. H. Nealson, Nonbiological fractionation of iron isotopes. *Science* 2000, 288, 126-128.
22. C. Lentner, in *Geigy Scientific Tables*. Ciba-Geigy Corporation Ciba-Geigy Limited, Basle, Switzerland: West Caldwell, New Jersey, USA, 8 edn., 1984, vol. 3, pp 84-85.
23. B. Copeland, P. Dyer, A. Pesce, Hemoglobin determination in plasma or serum by first-derivative recording spectrophotometry. Evaluation of the procedure of Soloni, Cunningham, and Amazon. *American journal of clinical pathology* 1989, 92, 619.
24. G. M. Brittenham, in *Iron Metabolism in Health and Disease*, ed. J. H. Brock, J. W. Halliday, M. J. Pippard, L. W. Powell. W.B. Saunders Company Ltd.: London, 1994, pp 31-62.
25. T. H. Bothwell, Absorption of iron. *Annual Reviews Medicine* 1970, 21, 145-156.
26. (a) K. Dideriksen, J. A. Baker, S. L. S. Stipp, Equilibrium Fe isotope fractionation between inorganic aqueous Fe(III) and the siderophore complex, Fe(III)-desferrioxamine B (vol 269, pg 280, 2008). *Earth and Planetary Science Letters* 2008, 272, 758-758, DOI: 10.1016/j.epsl.2008.06.001; (b) J. L. L. Morgan, L. E. Wasylenki, J. Nueter, A. D. Anbar, Fe Isotope Fractionation during Equilibration of Fe-Organic Complexes. *Environmental Science & Technology* 2010, 44, 6095-6101, DOI: 10.1021/es100906z.
27. G. R. Bakker, R. F. Boyer, Iron incorporation into apoferritin. The role of apoferritin as a ferroxidase. *J. Biol. Chem.* 1986, 261, 13182-13186.